

Sensitive SERS detection of Rhodamine 6G based on monodisperse Ag and Ag@SiO₂ nanocubes

Minh-Kha Nguyen^{1,2,*}, Lam-Nguyen Vo-Nguyen^{1,2}



Use your smartphone to scan this QR code and download this article

ABSTRACT

The sensitive detection of dye contaminants in aquatic environments is a critical issue for both ecological balance and human health. Surface-enhanced Raman scattering (SERS) using Au or Ag nanoparticles is commonly used for pollutant analysis. However, achieving precise control over nanoparticle size and shape during synthesis remains a major challenge. As a result, the sensitivity and reproducibility of Raman signals from these substrates are often insufficient for detecting low-level contaminants. In this study, monodisperse Ag nanocubes (Ag NCs) with uniform size were successfully controlled using the polyol method in combination with poly(vinylpyrrolidone). An ultrathin layer of silica was then coated onto the Ag NCs, forming Ag@SiO₂ NCs to enhance their chemical durability. The results exhibited that the SERS signal of 10⁻⁵ M Rhodamine 6G (R6G) on the Ag@SiO₂ NCs substrate was 3 times higher than that of Ag NCs. The SERS enhancement factor for R6G on Ag@SiO₂ NCs reached 1.3x10⁶. Furthermore, the silica shell of Ag@SiO₂ NCs maintained the stability of the R6G analytical signal even after 12 weeks of storage. The high sensitivity and stability of Ag@SiO₂ NCs demonstrate their strong potential for application in monitoring environmental pollutants.

INTRODUCTION

In recent years, the presence of dye in wastewater has become a significant environmental pollutant among industrial discharges. These harmful dye pollutants, typically originating from industries such as printing, textiles, leather, medicine, cosmetics, and food, are contributing water contamination and negatively impacting aquatic ecosystems¹. As a result, the detection of dyes is critical for both ecological preservation and safeguarding human health. Over the past few decades, a variety of techniques have been developed for detecting dye pollutants²⁻⁴, including UV-Vis spectroscopy, fluorescence spectroscopy, electro-analytical techniques, Raman spectroscopy, infrared spectroscopy, and mass-spectrometry. Among these methods, Raman spectroscopy has gained widespread use in chemistry and material science. However, its practical application is often limited by low sensitivity, making it necessary to enhance Raman signals to improve detection capabilities.

Within plasmonic technologies, optical nanostructures made of metals play crucial roles as light guides, precisely directing light to desired locations at the nanoscale, and as nanoantennas, which enhance electric fields. These functionalities arise from the strong interaction between incident light and free electrons within the nanostructures. Additionally, effective manipulation of light is achievable through precise

control over shape and sizes of the nanostructures⁵. Numerous innovative technologies stand to benefit from plasmonics, including invisibility cloaks⁶, superlens⁷, and quantum computing⁸. Moreover, surface-enhanced Raman spectroscopy (SERS) can also experience significant improvements in speed and efficiency through the integration of plasmonic nanostructures⁹. SERS has emerged as a key tool for amplifying the inherently weak Raman scattering of molecules, enabling specific and sensitive detection of analytes, which is critical for applications in disease diagnosis¹⁰, understanding protein functionality, and monitoring environmental pollutants¹¹.

Various nanostructures made of Au, Ag, and Cu, with controllable shapes and sizes, have been synthesized and are of considerable interest for SERS applications¹². However, Cu nanoparticles are unsuitable for such applications due to their susceptibility to air oxidation. While Au is significantly more expensive than Ag, Ag stands out among metals for its exceptional plasmonic properties, a wide variety of nanostructure options, and cost-effectiveness. Despite these advantages, Ag nanostructures face challenges related to poor chemical and structural stability. Under conditions such as acids, halides, oxidants, and heat, Ag nanostructures tend to undergo shape transformation into spherical particles¹³, leading to a blue shift in the

¹Faculty of Chemical Engineering, Ho Chi Minh City University of Technology (HCMUT), Vietnam

²Vietnam National University Ho Chi Minh City, Vietnam

Correspondence

Minh-Kha Nguyen, Faculty of Chemical Engineering, Ho Chi Minh City University of Technology (HCMUT), Vietnam

Vietnam National University Ho Chi Minh City, Vietnam

Email: nmkha@hcmut.edu.vn

History

- Received: 07-09-2024
- Revised: 24-03-2026
- Accepted: 25-03-2026
- Published Online: 28-03-2026

DOI : x



Check for updates

Copyright

© VNUHCM Journal. This is an open-access article distributed under the terms of the Creative Commons Attribution 4.0 International license.

Cite this article : Nguyen M, Vo-Nguyen L. Sensitive SERS detection of Rhodamine 6G based on monodisperse Ag and Ag@SiO₂ nanocubes. VNUHCM J. Eng. Technol, 2026, 9(1):2771-2777

surface plasmon resonance (SPR) band. This instability complicates the use of anisotropic Ag nanoparticles (NPs), particularly those with sharp edges, for plasmonic applications. To overcome these challenges, efforts to obtain stable anisotropic Ag nanostructures, such as nanocubes, triangles, or nanorods, while preserving their superior plasmonic characteristics for SERS applications are highly desirable. Additionally, concerns about the potential toxicity of Ag, particularly the released Ag^+ ions, pose significant limitations for in vivo applications¹⁴.

In this study, the structure and dimensions of Ag nanocubes (NCs) were controlled using the polyol technique. To enhance the stability of Ag NCs, a uniform silica layer with ultra thin shell was developed through the Stöber condensation reaction, effectively coating the Ag NCs. Both Ag and Ag@SiO_2 NCs-based substrates exhibited remarkable stability and uniformity, providing highly effective for the detection of Rhodamine 6G (R6G). These substrates show significant potential for environmental monitoring, particularly for assessing water contamination.

MATERIALS AND METHODS

Materials

Poly(vinylpyrrolidone) (PVP, $M_w \approx 55000$), Rhodamine 6G, (3-aminopropyl)trimethoxysilane (APTMS), and hydrochloric acid were acquired from Sigma-Aldrich. Silver trifluoroacetate, sodium hydrosulfide, ethylene glycol (EG), tetraethyl orthosilicate (TEOS), and acetone were procured from Acros. Ammonium hydroxide and isopropanol (IPA), each of analytical grade, were sourced from Fisher. For all experiments, deionized (DI) water was utilized.

Synthesis of Ag NCs

The preparation of Ag NCs was conducted according to our previously established protocol¹⁵, with slight adjustments. The scaling up of Ag NC synthesis was executed by adhering to the standard synthesis procedure, albeit with quadruple the amount of all reagents (Figure 1). Following specific reaction periods, the reaction solution was halted by cooling in an ice-water bath. The Ag NCs were collected via centrifugation, washed with acetone and ethanol, dispersed in IPA, and stored at 4 °C.

Synthesis of Ag@SiO_2 NCs

A volume of 20 μL of APTMS (1mM in IPA) was introduced to 2 mL of Ag NCs solution and stirred at room temperature for 30 min. Subsequently, 6 mL

of IPA, 2 mL of DI water, and 100 μL of ammonia aqueous solution were supplemented to the mixture. A dropwise addition of 200 μL of TEOS (1mM in IPA) ensued, and the reaction proceeded for 6 h. The Ag@SiO_2 NCs were collected via centrifugation, washed with ethanol and DI water, dispersed in DI water, and stored at 4 °C.

Characterizations

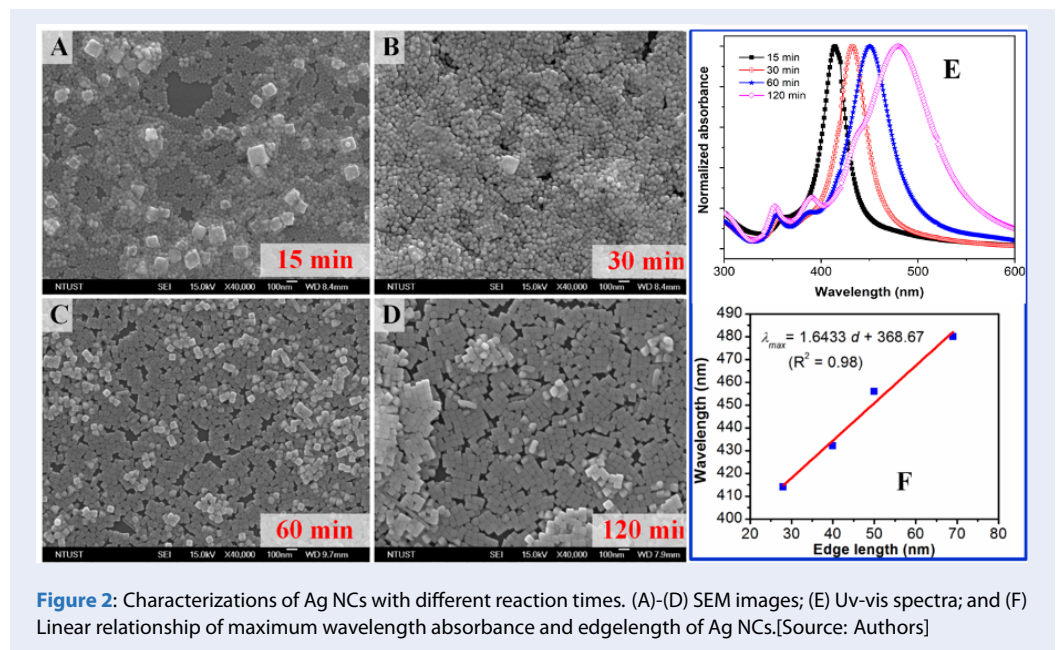
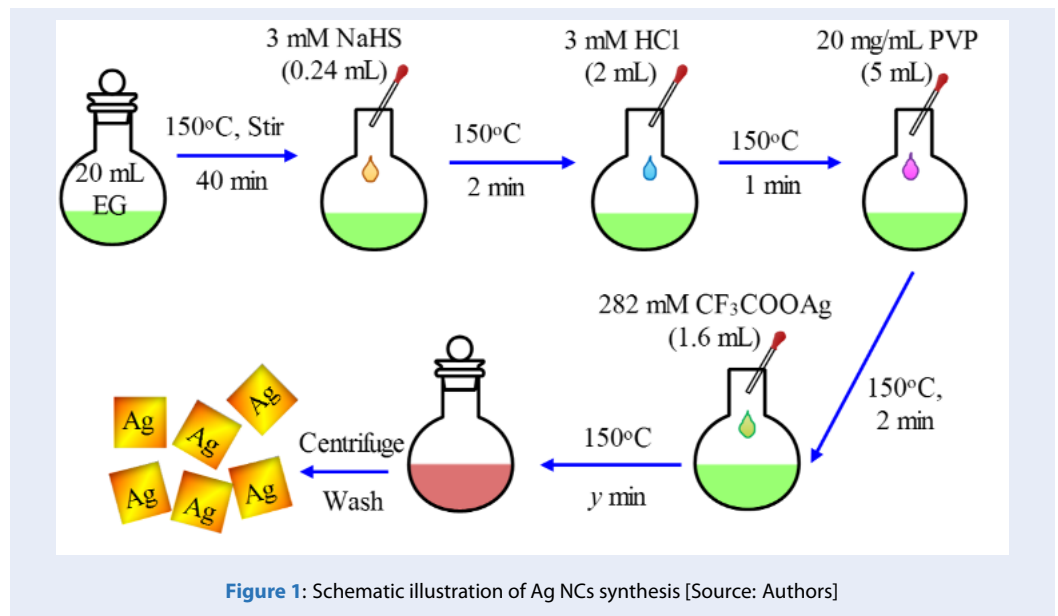
UV-Vis absorption spectra of the solution were carried out using UV-750, Jasco. The surface structures of nanoparticles were analyzed by FESEM (JSM-6500F, JEOL) and TEM (FEI Tecnai 20 G2 S-Twin). For SERS measurements, a 20 μL solution of Ag@SiO_2 NCs or Ag NCs was dropped on a Si substrate. A 5 μL of 10^{-5} M R6G was applied to the substrate and left in darkness for 1 h at room temperature. SERS measurements were conducted using a UniRAM micro-Raman spectrometer and a laser power of ~ 1.5 mW with a wavelength of 532 nm. Five spectra of SERS signals were measured for each sample.

RESULTS

In order to explore the impact of size effects of Ag NCs on localized surface plasmon resonance (LSPR) and Raman enhancement, Ag NCs were synthesized through various reaction durations. Analysis of the SEM images depicted in Figure 2A-D reveals that the average edge length (d) of Ag NCs, synthesized at different reaction time: 15, 30, 60, and 120 min, respectively, exhibited an increase from 28 to 40, 50, and 69 nm. Furthermore, the phenomenon of agglomeration is observed in smaller sizes (Figure 2A-B) due to a higher relative surface area and a greater number of surface atoms¹⁶.

The investigation into the correlation between the plasmon shifts and the nanoparticle size involved presenting the relationship between various edge lengths and the LSPR peak positions of Ag NCs solutions in Figure 2E through UV-vis spectra. The primary LSPR peaks (λ_{max}) of the Ag NCs demonstrated a shift towards longer wavelengths from 414 to 432, 456, and 480 nm while concurrently experiencing significant broadening with an increase in edge lengths. The SERS sensitivity of the synthesized Ag NCs was assessed using R6G as a representative Raman probe (Figure 3).

The TEM results displayed in Figure 4A-B exhibit well-dispersed Ag and Ag@SiO_2 core-shell NCs. The produced Ag particles are monodisperse cubic in shape, with edge lengths of approximately 50 nm. By employing APTMS and TEOS through the Stöber



process, a uniformly thin silica shell (~1.5 nm thick) was coated on the Ag NCs (Figure 4B). The UV-Vis spectra of the Ag NCs (Figure 4C) revealed a predominant band with a peak at 457 nm, representing the dipole resonance of the NCs in solution. Additionally, higher order resonances were observed in the solution spectrum at 355 nm and 390 nm, indicating a multipolar resonance and a hybrid quadrupolar resonance, respectively¹⁷. Upon the application of a uniform SiO₂ shell on the Ag NCs, the localized surface plasmon resonance peak experienced a slight red-shift

from 457 nm to 464 nm due to the increased dielectric constant resulting from the SiO₂ layer formation on Ag NCs' surface. The spectral redshift observed is attributed to the rising dielectric constant of the environment and the accumulation of polarization charges on the dielectric side of the interface, which weakens the restoring force within the nanoparticles. Another critical aspect influencing the viability of the nanocubes as a label-free SERS detection method in the environment is their long-term stability. The sensitivity and stability of the Ag NCs and Ag@SiO₂ NCs

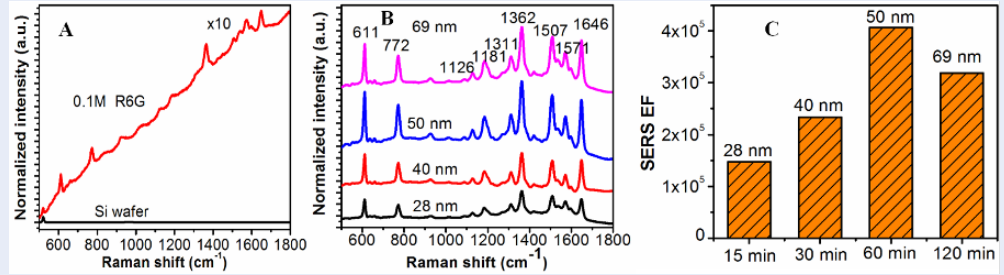


Figure 3: Raman spectra with the excitation laser 532 nm of: (A) silicon wafer and 0.1 M R6G on a silicon substrate (10 times); (B) SERS intensity and (C) SERS EF of 10⁻⁵ M R6G on Ag NCs synthesized with various sizes. [Source:Authors]

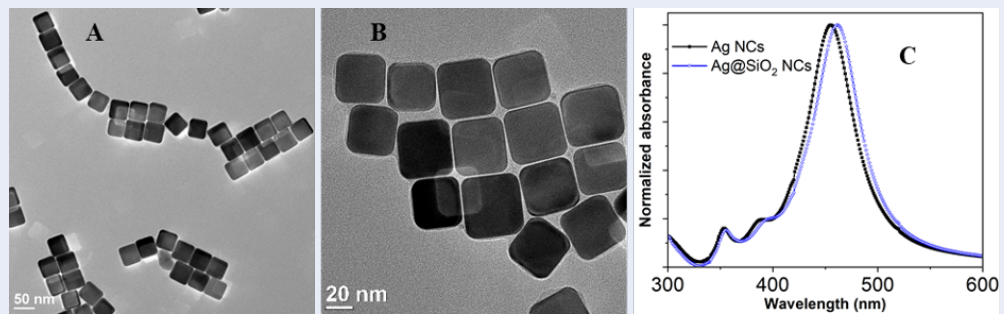


Figure 4: TEM images of (A) AgNCs and (B) Ag@SiO₂ NCs. (C) Uv-vis spectra. [Source:Authors]

were evaluated for detecting R6G. As showed in Figure 5, the Raman signal of R6G on prepared Ag@SiO₂ NCs was three times higher than that on bare Ag NCs.

DISCUSSIONS

As shown in Figure 2, the redshift observed in larger NCs is attributed to a decrease in the depolarization field due to retardation effects. These effects cause the conduction electrons to become desynchronize in motion, resulting in a weaker depolarization field at the particle’s center, which is induced by the surrounding polarized medium¹⁸. Additionally, radiative losses begin to play a significant role in plasmon damping, eventually dominating the damping process entirely in Au and Ag NPs with diameters exceeding 100 nm¹⁹. This leads to a broadening of the resonance peak. The relatively slow growth rate during synthesis enabled precise control over the sizes of the resulting Ag NCs, as indicated by their LSPR peak. Figure 2F shows a linear relationship between the LSPR peak position and the edge length of the Ag NCs. The calibration curve is described by the equation:

$$\lambda_{max} = 1.6433d + 368.67 (R^2 = 0.98)$$

where λ_{max} and d represent the peak position and edge length, respectively. This calibration curve can

be practically to predict the specific edge length of Ag NCs by monitoring their UV-vis spectra.

The enhancement of Raman signal is crucial, making the enhancement factor (EF) as a key metric for evaluating the effectiveness of the SERS substrate. The EF is calculated using the equation $EF = 1.19 \times 10^4 \times \frac{I_{SERS}}{I_{ref}}$, where I_{SERS} and I_{ref} represent the intensities of the selected band at 611 cm⁻¹, recorded by SERS and on the silicon wafer, respectively (Figure 3A).

In general, plasmonic NPs with dimensions in the range of ~30 – 100 nm exhibit significant size effects. This is because their size constitutes a substantial fraction of the wavelength at maximum absorbance, affecting the extinction cross-section. Analyzing the influence of size on LSPR is complex and typically requires the numerical solution of Maxwell’s equations. The size effects can be qualitatively summarized as follows: as nanoparticle size increases, the LSPR redshifts and becomes strongly damped, primarily due to increased radiation losses. This damping leads to a broadening of the resonance, an increase in bandwidth, and a substantial reduction in the associated local electromagnetic field. Conversely, for small particles, the electrostatic approximation is sufficient, and the resonance effects do not occur. For

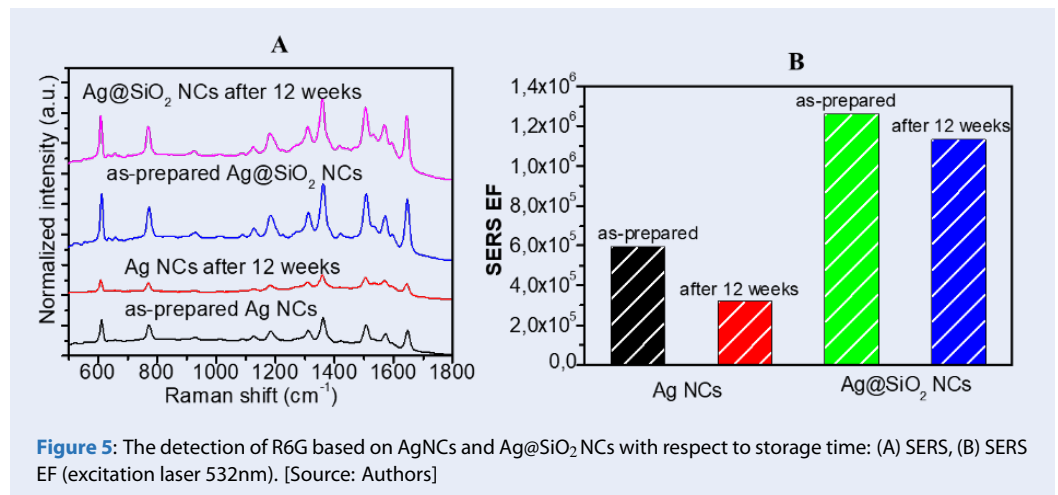


Figure 5: The detection of R6G based on AgNCs and Ag@SiO₂ NCs with respect to storage time: (A) SERS, (B) SERS EF (excitation laser 532nm). [Source: Authors]

the same particle shape, size-dependent resonances, such as multipolar resonances (e.g., quadrupolar resonances at the particle edges), become more prominent. However, in small particles, these resonances cannot effectively couple to light, and the surface plasmon band may disappear entirely. Additionally, it is well-known that depolarization field and additional damping mechanisms in small particles reduce the enhancement of the excitation field (5). As a result, smaller Ag NCs exhibit a lower SERS EF compare to larger NCs. By balancing LSPR oscillations and the resonant coupling with the excitation laser, the highest SERS EF was observed for Ag NCs of approximately 50 nm, corresponding to a reaction time of 60 min. Moreover, the SERS EF for the detection of R6G in Figure 5 was determined to be 1.3×10^6 for the Ag@SiO₂ NCs. Following a 12-week storage period, the SERS sensitivity of the Ag NCs significantly decreased by ~47%, whereas the enhancement factor of the Ag@SiO₂ NCs remained over 90% of the initial values. The commercially available SERS substrate, such as Klarite™, consists of a ~300 nm thick gold layer coated on arrays of inverted square pyramids etched in silicon. While this substrate remains costly, the SERS EFs range from 10^3 to 10^6 , depending on the type of molecule being detected²⁰. In contrast, common SERS substrates like AgNPs or AuNPs typically retained only about 30% of their initial performance after 2 months of storage²¹. A silica coating creates a controlled dielectric environment around Ag NPs²², enhancing the precision of SPR-based sensing. Additionally, the coating protects the nanoparticles by preventing or slowing the diffusion of environmental oxygen, thereby increasing their stability. Since silica is chemically inert, it does not interfere with redox

reactions occurring on the core's surface, preserving the functionality of the Ag NPs. The silica coating on Ag NCs not only enhances their chemical durability and stability but also promotes efficient interaction with a wide range of dye molecules, making them versatile for broad-spectrum pollutant detection. Additionally, the silica layer increases the SERS EF by creating a controlled dielectric environment and enhancing local electric fields around the Ag NCs, further improving the sensitivity of the detection process.

CONCLUSIONS

In this study, Ag NCs with well-controlled sizes and sharp corners/edges were successfully synthesized using the polyol method. By balancing the two key factors influencing LSPR oscillations in metallic NPs – radiation damping of surface plasmons (predominant in large NPs) and resonant coupling of surface plasmon oscillations with excitation laser (stronger in smaller NPs), Ag NCs with an edge length of ~50 nm were identified as the optimal size for maximizing SERS enhancements. Furthermore, a method for fabricating ultrathin silica-coated Ag NCs using the coupling agent APTMS was proposed. The ultrathin silica shell provides several advantages, including preserving the anisotropic structures of Ag NCs, enhancing local electric fields, and reducing the quenching effect in SERS. Additionally, the silica coating inhibits oxygen diffusion and reduces the cytotoxicity of Ag NCs, maintaining their stability and functionality even after a 12-week storage periods. These characteristics demonstrate that Ag@SiO₂ NCs are exceptional substrate for SERS applications, particularly in environmental monitoring and biological analyses.

ACKNOWLEDGEMENTS

This research is funded by Vietnam National University Ho Chi Minh City (VNU-HCM) under grant number C2024-20-20. The authors are grateful to the support of facilities from Ho Chi Minh City University of Technology (HCMUT), VNU-HCM for the research and Prof. Bing-Joe Hwang for his kind assistance in SERS characterization.

AUTHOR CONTRIBUTIONS

Minh-Kha Nguyen contributed to conceptualization, methodology, experimental investigation, data analysis, and manuscript writing and editing. Lam-Uyen Vo-Nguyen provided support for manuscript writing. All authors reviewed and approved the final version of the manuscript.

REFERENCES

- Al-Tohamy R, Ali SS, Li F, Okasha KM, Mahmoud YA, Elsamahy T, et al. A critical review on the treatment of dye-containing wastewater: ecotoxicological and health concerns of textile dyes and possible remediation approaches for environmental safety. *Ecotoxicology and Environmental Safety*. 2022;231. Available from: <https://doi.org/10.1016/j.ecoenv.2021.113160>.
- Katheresan V, Kansedo J, Lau SY. Efficiency of various recent wastewater dye removal methods: A review. *Journal of Environmental Chemical Engineering*. 2018;6(4):4676–97. Available from: <https://doi.org/10.1016/j.jece.2018.06.060>.
- Okeke ES, Ezeorba TP, Okoye CO, Chen Y, Mao G, Feng W, et al. Analytical detection methods for azo dyes: A focus on comparative limitations and prospects of bio-sensing and electrochemical nano-detection. *Journal of Food Composition and Analysis: An Official Publication of the United Nations University, International Network of Food Data Systems*. 2022;114. Available from: <https://doi.org/10.1016/j.jfca.2022.104778>.
- Idris AO, Orimolade B, Dennany L, Mamba B, Azizi S, Kaviyarasu K, et al. A Review on Monitoring of Organic Pollutants in Wastewater Using Electrochemical Approach. *Electrocatalysis (New York)*. 2023;14(5):659–87. Available from: <https://doi.org/10.1007/s12678-023-00834-x>.
- Brongersma ML, Shalae VM. Applied physics. The case for plasmonics. *Science*. 2010;328(5977):440–1. Available from: <https://doi.org/10.1126/science.1186905>.
- Galutin Y, Falek E, Karabchevsky A. Invisibility Cloaking Scheme by Evanescent Fields Distortion on Composite Plasmonic Waveguides with Si Nano-Spacer. *Scientific Reports*. 2017;7(1):12076. Available from: <https://doi.org/10.1038/s41598-017-10578-6>.
- Li H, Fu L, Frenner K, Osten W. Design studies of a far-field plasmonic superlens with an enlarged field of view. *Optical Materials*. 2023;138. Available from: <https://doi.org/10.1016/j.optmat.2023.113688>.
- Liu Y, Zhou H, Xue P, Lin L, Sun HB. Photoswitchable quantum electrodynamics in a hybrid plasmonic quantum emitter. *Chip (W&#amp;#x00FC;rzburg)*. 2023;2(3). Available from: <https://doi.org/10.1016/j.chip.2023.100060>.
- Xiao X, Gillibert R, Foti A, Coulon PE, Ulysse C, Levato T, et al. Plasmonic Polarization Rotation in SERS Spectroscopy. *Nano Letters*. 2023;23(7):2530–5. Available from: <https://doi.org/10.1021/acs.nanolett.2c04461>.
- Chen Y, Zheng S, Tang X, Wang F, Wang L, Li C. Recent Research Progress of Surface-Enhanced Raman Scattering Dominated Analysis Strategies in Early Diagnosis of Diseases. *Chemistry, an Asian Journal*. 2023;18(12). Available from: <https://doi.org/10.1002/asia.202300264>.
- Kitaw SL, Birhan YS, Tsai HC. Plasmonic surface-enhanced Raman scattering nano-substrates for detection of anionic environmental contaminants: current progress and future perspectives. *Environmental Research*. 2023;221. Available from: <https://doi.org/10.1016/j.envres.2023.115247>.
- Xia Y, Xiong Y, Lim B, Skrabalak SE. Shape-controlled synthesis of metal nanocrystals: simple chemistry meets complex physics? *Angewandte Chemie International Edition in English*. 2009;48(1):60–103. Available from: <https://doi.org/10.1002/anie.200802248>.
- Kalachyova Y, Mares D, Jerabek V, Elashnikov R, Švorik V, Lyutakov O. Longtime stability of silver-based SERS substrate in the environment and (bio)environment with variable temperature and humidity. *Sensors and Actuators A, Physical*. 2019;285:566–72. Available from: <https://doi.org/10.1016/j.sna.2018.11.037>.
- Skvortsov AN, Ilyechova EY, Puchkova LV. Chemical background of silver nanoparticles interfering with mammalian copper metabolism. *Journal of Hazardous Materials*. 2023;451. Available from: <https://doi.org/10.1016/j.jhazmat.2023.131093>.
- Nguyen MK, Su WN, Hwang BJ. A Plasmonic Coupling Substrate Based on Sandwich Structure of Ultrathin Silica-Coated Silver Nanocubes and Flower-Like Alumina-Coated Etched Aluminum for Sensitive Detection of Biomarkers in Urine. *Advanced Healthcare Materials*. 2017;6(10). Available from: <https://doi.org/10.1002/adhm.201601290>.
- Elzey S, Grassian VH. Agglomeration, isolation and dissolution of commercially manufactured silver nanoparticles in aqueous environments. *Journal of Nanoparticle Research*. 2010;12(5):1945–58. Available from: <https://doi.org/10.1007/s11051-009-9783-y>.
- Bottomley A, Prezgot D, Coyle JP, Ianoul A. Dynamics of nanocubes embedding into polymer films investigated via spatially resolved plasmon modes. *Nanoscale*. 2016;8(21):11168–76. Available from: <https://doi.org/10.1039/C6NR02604D>.
- Meier M, Wokaun A. Enhanced fields on large metal particles: dynamic depolarization. *Optics Letters*. 1983;8(11):581–3. Available from: <https://doi.org/10.1364/OL.8.000581>.
- Wokaun A, Gordon JP, Liao PF. Radiation Damping in Surface-Enhanced Raman Scattering. *Physical Review Letters*. 1982;48(14):957–60. Available from: <https://doi.org/10.1103/PhysRevLett.48.957>.
- Chin-Heng L, Chun-Hung T, Ding-Zheng L. Optimization of physical vapor deposition process for low background nanoimprinted SERS substrate in quantitative melamine analysis. *Spectrochimica Acta Part A, Molecular and Biomolecular Spectroscopy*. 2024;306. Available from: <https://doi.org/10.1016/j.saa.2023.123563>.
- Pérez-Jiménez AI, Lyu D, Lu Z, Liu G, Ren B. Surface-enhanced Raman spectroscopy: benefits, trade-offs and future developments. *Chemical Science (Cambridge)*. 2020;11(18):4563–77. Available from: <https://doi.org/10.1039/D0SC00809E>.
- Wang X, Wang X, Liu Y, Chu T, Li Y, Dai C, et al. Surface plasma enhanced fluorescence combined aptamer sensor based on silica modified silver nanoparticles for signal amplification detection of cholic acid. *Microchemical Journal: Devoted to the Application of Microtechniques in All Branches of Science*. 2021;168. Available from: <https://doi.org/10.1016/j.micro.2021.106524>.

Phát hiện Rhodamine 6G độ nhạy cao bằng SERS dựa trên nano lập phương Ag và Ag@SiO₂ đơn phân tán

Nguyễn Minh Kha^{1,2,*}, Võ Nguyễn Lam Uyên^{1,2}



Use your smartphone to scan this QR code and download this article

TÓM TẮT

Việc phát hiện các chất màu ô nhiễm trong môi trường nước với độ nhạy cao có ý nghĩa quan trọng đối với cân bằng sinh thái và sức khỏe con người. Phương pháp tán xạ Raman tăng cường bề mặt (SERS) sử dụng các hạt nano Au hoặc Ag thường được dùng trong phân tích chất ô nhiễm. Tuy nhiên, việc kiểm soát chính xác kích thước và hình dạng hạt nano trong quá trình tổng hợp vẫn còn nhiều thách thức, dẫn đến độ nhạy và tính lặp lại của tín hiệu Raman chưa cao, đặc biệt ở nồng độ thấp của chất cần phân tích. Trong nghiên cứu này, các hạt nano bạc đơn phân tán dạng lập phương (Ag NCs) có kích thước đồng đều đã được tổng hợp thành công bằng phương pháp polyol kết hợp với poly(vinylpyrrolidone). Tiếp đó, một lớp silica siêu mỏng được phủ lên bề mặt, tạo thành cấu trúc Ag@SiO₂ NCs nhằm tăng độ bền hóa học. Kết quả cho thấy tín hiệu SERS của Rhodamine 6G (R6G) ở nồng độ 10⁻⁵ M trên nền Ag@SiO₂ NCs cao gấp ba lần so với Ag NCs, với hệ số tăng cường đạt 1,3 × 10⁶. Đồng thời, lớp vỏ silica giúp duy trì độ ổn định của tín hiệu phân tích R6G sau 12 tuần lưu trữ. Những kết quả này cho thấy Ag@SiO₂ NCs có độ nhạy và độ ổn định cao, hứa hẹn tiềm năng ứng dụng trong giám sát các chất ô nhiễm môi trường.

Từ khoá: Ag@SiO₂, Rhodamine 6G, plasmon, giám sát môi trường, chất màu ô nhiễm

¹Khoa Kỹ thuật Hóa học, Trường Đại học Bách khoa Tp. HCM (HCMUT), Việt Nam

²Đại học Quốc gia Thành phố Hồ Chí Minh, Việt Nam

Liên hệ

Nguyễn Minh Kha, Khoa Kỹ thuật Hóa học, Trường Đại học Bách khoa Tp. HCM (HCMUT), Việt Nam

Đại học Quốc gia Thành phố Hồ Chí Minh, Việt Nam

Email: nmkha@hcmut.edu.vn

Lịch sử

- Ngày nhận: 07-09-2024
- Ngày sửa đổi: 24-03-2026
- Ngày chấp nhận: 25-03-2026
- Ngày đăng: 28-03-2026

DOI: x



Bản quyền

© Tạp chí ĐHQG-HCM. Đây là bài báo công bố mở được phát hành theo các điều khoản của the Creative Commons Attribution 4.0 International license.

Trích dẫn bài báo này: Minh Kha N, Lam Uyên V N. **Phát hiện Rhodamine 6G độ nhạy cao bằng SERS dựa trên nano lập phương Ag và Ag@SiO₂ đơn phân tán.** VNUHCM J. Eng. Technol, 2026, 9(1):2771-2777

Bài báo này được xuất bản trong giai đoạn tạp chí đang đổi tên từ Tạp chí Phát triển Khoa học và Công nghệ - Kỹ thuật và Công nghệ 2777 (ISSN: 2615-9872) sang VNUHCM Journal of Engineering and Technology; ISSN mới hiện đang chờ được cấp.